



HAL
open science

An algorithm to decompose ground reaction forces and moments from a single force platform in walking gait

David Villeger, Antony Costes, Bruno Watier, Pierre Moretto

► To cite this version:

David Villeger, Antony Costes, Bruno Watier, Pierre Moretto. An algorithm to decompose ground reaction forces and moments from a single force platform in walking gait. *Medical Engineering & Physics*, 2014, 36 (11), pp.1530-1535. 10.1016/j.medengphy.2014.08.002 . hal-01662980

HAL Id: hal-01662980

<https://laas.hal.science/hal-01662980v1>

Submitted on 13 Dec 2017

HAL is a multi-disciplinary open access archive for the deposit and dissemination of scientific research documents, whether they are published or not. The documents may come from teaching and research institutions in France or abroad, or from public or private research centers.

L'archive ouverte pluridisciplinaire **HAL**, est destinée au dépôt et à la diffusion de documents scientifiques de niveau recherche, publiés ou non, émanant des établissements d'enseignement et de recherche français ou étrangers, des laboratoires publics ou privés.

1 Technical Note

2 **An algorithm to decompose ground reaction forces and moments**
3 **from a single force platform in walking gait**

4 **Authors:**

5 David Villeger^a, Antony Costes^a, Bruno Watier^{a, b} and Pierre Moretto^a

6 **Affiliation:**

7 ^a University of Toulouse, UPS, PRISSMH, 118 route de Narbonne, F-31062 Toulouse Cedex
8 9, France

9 ^b CNRS ; LAAS ; 7 avenue du colonel Roche, F-31077 Toulouse, France

10

11 **Corresponding author:**

12 David Villeger

13 PRISSMH

14 Faculté des Science du Sport et du Mouvement Humain (F2SMH)

15 Université de Toulouse III, 118 route de Narbonne, F-31062 Toulouse Cedex 9, France.

16 Phone: +33 (0)6 51 49 11 58 / +33 (0)5 61 55 64 40

17 Fax: +33 (0)5 61 55 82 80

18 Email: david.villeger@univ-tlse3.fr

19 **Word count (abstract):** 250 words

20 **Word count (Introduction through References with appendix):** 2861 words

21 **Number of figure:** 5 figures

22 **Number of table:** 2 tables

23

24 **An algorithm to decompose ground reaction forces and moments from a**
25 **single force platform in walking gait**

26 **Abstract**

27 In walking experimental conditions, subjects are sometimes unable to perform two
28 steps on two different forceplates. This leads the authors to develop methods for discerning
29 right and left ground reaction data while they are summed during the double support in
30 walking. The aim of this study is to propose an adaptive transition function that considers the
31 walking speed and ground reaction forces (GRF). A transition function is used to estimate left
32 and right side GRF signals in double support. It includes a shape coefficient adjusted using
33 single support GRF parameters. This shape coefficient is optimized by a non-linear least-
34 square curve-fitting procedure to match the estimated signals with real GRF. A multiple
35 regression is then performed to identify GRF parameters of major importance selected to
36 compute the right and left GRF of the double support. Relative RMSE ($RMSE_R$), maximum
37 GRF differences normalized to body mass and differences of center of pressure (CoP) are
38 computed between real and decomposed signals. During double support, $RMSE_R$ are 6%,
39 18%, 3.8%, 4.3%, 3%, and 12.3% for anterior force, lateral force, vertical force, frontal
40 moment, sagittal moment and transverse moment, respectively. Maximum GRF differences
41 normalized to body mass are lower than 1N/kg and mean CoP difference is 0.0135 m, when
42 comparing real to decomposed signals during double support. This work shows the accuracy
43 of an adaptive transition function to decompose GRF and moment of right and left sides. This
44 method is especially useful to accurately discern right and left GRF data in single force
45 platform configurations.

46

47 **Keywords:** Double support detection; double support decomposition; center of pressure;
48 single forceplate; asymmetry.

49 **1. Introduction**

50 A common problem met with in walking analysis is that the subject may be unable to
51 perform two steps on two force platforms. Constrained by the experimental conditions, the
52 number and the size of the force platform, subjects have to respect a minimum step length
53 maintaining a natural behavior. Some authors have suggested methods using a single force
54 platform to study walking gait cycle [1–4].

55 Using a single force platform, measurements match the sum of the action forces.
56 However, the discrimination of right and left action forces and moments is required to study
57 walking gait using inverse dynamic and asymmetry analysis [5,6]. The difficulty with using a
58 single platform is to detect the Double Support (DS) phase and to decompose the whole
59 signals into left and right body parts. To identify heel strike and toe off of each foot, some
60 studies proposed to use the lateral Center of Pressure (CoP) position [2] or the forward CoP
61 speed [7]. Based on the DS detection, the whole signals can be decomposed.

62 Two options can be used to distinguish right to left action forces and moments. In the
63 first, an algorithm is carried out using the four load cells of a forceplate [1,2]. However,
64 access to the different load cells is not always possible depending on which platform is used.
65 Moreover, these studies are limited to the determination of the right and the left vertical
66 components of the Ground Reaction Force (GRF). The second option involves decomposing
67 GRF and Moments (GRM). This allows us to estimate the shape of the signal corresponding
68 to those of the right and left foot contact [8]. Ren et al. used transition functions to estimate
69 decreases in three dimensional forces and moments applied by the foot leaving the ground
70 during DS phase. These transition functions were developed to respect two conditions in the
71 DS phase:

72 (1) The GRF and the GRM on the leaving foot change towards zero.

73 (2) The ratio of GRF and GRM during DS to their values at contralateral heel strike can be

74 expressed as a function of DS duration.

75 However, Ren's method allowed them to use only two shapes of signal decrease.

76 The shapes of the ground reaction force and moment being walking-speed dependent
77 [9], this study aims to enhance the transition functions of Ren et al. [8] by including pre-DS
78 ground reaction force characteristics and taking into account the walking speed to determine
79 three dimensional forces and moments of both right and left sides.

80

81 **2. Methods**

82 **2.1. Walking test**

83 Seven healthy subjects with a mean age (SD) of 23.4 (3.5) yr; a height (SD) of 1.73
84 (0.07) m and a body mass (SD) of 72.1 (6) kg took part in the study after signing an informed
85 consent document. They performed walking tests at three different velocities: low 1.1 (0.13)
86 m/s, normal 1.4 (0.1) m/s and high speed 1.9 (0.15) m/s on a walkway including two force
87 plates (AMTI, Watertown, MA, USA). Twelve infrared cameras (Vicon, Oxford Metrics,
88 Oxford, UK) were used to measure the subject walking speed. They performed ten trials per
89 walking condition after a familiarization period to ensure data reproducibility [10]; hence 210
90 trials were recorded for this study. The kinematic and force platform data were sampled at
91 200Hz and 1000Hz, respectively. Note that AMTI forceplate did not enable us to discriminate
92 the four load cells.

93

94 **2.2. Assessed and computed parameters**

95 *Assessed parameters*

96 X, Y and Z were respectively anterior, lateral and vertical axis. The forward velocity
97 was measured from a virtual point corresponding to the middle of two markers placed at both
98 anterior iliac spines. The GRF and GRM of both platforms were transferred to a corner of the

99 first platform. Then, to simulate single data recordings, data of the two force platforms were
100 summed and then filtered. 4th order zero lag Butterworth filters with a cut off frequency of
101 10Hz [11] were applied to kinematic and kinetic data. The GRF and GRM transfers also
102 allowed to improve the GRM decompositions because of no sign changes.

103 *Computed parameters*

104 Referring to Verkerke et al. [7], the transitions from the single to the double stance
105 and from the double to the single stance were estimated when the forward CoP speed reached
106 the zero level. As the authors used a treadmill, we decided to subtract the mean subject
107 forward speed on the cycle from the forward CoP velocity (Fig. 1), to match their procedure
108 and detect DS phase events. CoPx and CoPy were computed from the ratios $-My/Fz$ and
109 Mx/Fz (with Mx the frontal moment, My the sagittal moment and Fz the vertical force),
110 respectively. The determination of DS events from two force platforms was detected with a
111 threshold of 5N on vertical force [12].

112

113 PLEASE INSERT FIGURE 1

114

115 The transition function used in this paper has been optimized with respect to the
116 original used by Ren et al. [8] (Eq. 1). The transition function allows us to estimate the force
117 decrease of the foot leaving the ground during DS from the force recorded one frame before
118 DS. The force shape decrease depended on the GRF and GRM components. Indeed, Ren et
119 al. [8] suggested two shapes of decrease in the DS phase; i) a non monotonic (Fig. 2A) which
120 corresponded to an alternation of positive and negative variations and ii) a monotonic (Fig.
121 2A). They suggested using equation 1 to estimate anterior ground reaction force decrease
122 (non monotonic) and a monotonic transition function to estimate the other ground reaction
123 force and moment decreases.

$$F(t) = F_0 \cdot \left(k_1 \cdot e^{-[(t-t_p)/T_{ds}]^2} - k_2 \cdot \frac{t}{T_{ds}} \right) \quad (1)$$

124

125 According to Ren et al. [8], F_0 is the force at contralateral heel strike at the frame before the
 126 beginning of DS; T_{ds} is the half DS duration; t is the time ($t = 0$ at the frame before DS
 127 beginning and $t=2T_{ds}$ at DS end); $t_p = \text{Scoeff} \cdot T_{ds}$ with Scoeff the shape coefficient. Both
 128 constants $k_1 = e^{\text{Scoeff}^2}$ and $k_2 = (k_1/2) \cdot e^{-(2-\text{Scoeff})^2}$ allow the function to respect condition at
 129 contralateral heel strike ($F(0) = F_0$) and toe off ($F(2T_{ds})=0$). In the original non-monotonic
 130 transition function (Eq. 1) proposed by Ren et al. [8], the Scoeff was fixed at 2/3 (Fig. 2A).

131

132 PLEASE INSERT FIGURE 2

133

134 For a more accurate adaptation of Scoeff (Fig. 2B), we retain the non-monotonic
 135 transition function (Eq. 1) for all GRF and GRM. The optimization was performed to adjust
 136 Scoeff, GRF and GRM shapes from GRF characteristics and subject speed. The procedure
 137 comprises two steps (Fig. 2B), i) the Scoeff was optimized to best fit decomposed GRF and
 138 GRM to real GRF and GRM (see 2.3), ii) a multiple regression was performed to express
 139 optimized Scoeff in terms of pre-DS ground reaction force characteristics (see 2.4). The third
 140 figure shows a set of possible signal shapes by varying Scoeff in Eq. 1 which is the single
 141 transition function used in our method.

142

143 PLEASE INSERT FIGURE 3

144

145 **2.3. Optimized shape coefficient**

146 The Scoeff coefficient establishing the force at contralateral heel strike to decomposed
 147 GRF and GRM relation was first optimally estimated by means of a nonlinear unconstrained

148 least-square curve-fitting procedure using data relating to the two forceplates. For each
149 ground reaction component (force and moment), the optimization problem was formulated as:
150 Find Scoeff that minimizes:

$$151 \quad A_F = \sum_t (F_{REAL}(t) - F(t))^2 \quad (2)$$

152 where $F_{REAL}(t)$ is the real ground reaction component and $F(t)$ is obtained from equation 1 for
153 the corresponding ground reaction component. The optimization procedure was realized by
154 using the function `fminsearch` found in MATLAB and Optimization Toolbox (R2007b, The
155 MathWorks, Inc., Natick, Massachusetts, United States).

156

157 **2.4. GRF characteristics and multiple regression**

158 A multiple regression was then performed to express optimized Scoeff from GRF
159 characteristics. This determination allows us to calculate the optimized coefficient of each
160 recording using a single force plate. Different GRF parameters were taken into account to
161 identify their power in the determination of the optimized Scoeff. Their powers were
162 determined using a multiple regression analysis ($p < 0.05$) which takes into consideration:
163 F_{SLOPE} , the slope of absolute force normalized to body mass (BM) from the two frames before
164 the beginning of DS; F_i , the absolute force normalized to BM at the frame before the start of
165 DS; F_{MAX} , the absolute value of maximal force normalized to BM; $2T_{ds}$, the duration of DS
166 phase and V_F , the subject forward velocity. Significant parameters revealed by regression
167 analysis were taken into consideration to compute optimized Scoeff for each GRF and GRM.
168 Hence the signal decomposition shape from our method is dependent on Scoeff, while the
169 optimized Scoeff coefficient came from the multiple regression.

170 Ground reaction forces and moments under the foot striking the ground were obtained
171 by subtracting the decomposed ground reaction forces and moments to the total ground

172 reaction forces and moments.

173

174 **2.5. Computation error**

175 First, the times of heel strike and toe off that determine the DS phase were compared
176 with regard to two conditions: one simulated forceplate and two forceplates (see 2.2). The
177 two forceplates configuration was taken as a standard, and then the absolute error (in
178 seconds) was computed with the single forceplate configuration.

179 To evaluate model accuracy, decomposed GRF and GRM from our method and
180 decomposed GRF and GRM from the Ren's method were compared to the measured GRF
181 and GRM for each trial. Comparison is limited to the DS phase. The differences between both
182 methods and the real GRF and GRM were quantified by using the square root of the time-
183 averaged squared error, normalized with respect to mean peak-to-peak amplitude, $RMSE_R$
184 [8,13]. $RMSE_R$ of GRM being dependant on the coordinate system position, an error on CoP
185 for each trial was assessed. It entailed measuring the norms of the vectors between real CoP
186 and decomposed CoP from our method and Ren's method. A mean error (in meters) was
187 computed for each trial and for each decomposition method.

188 Maximum GRF differences (Δ) were computed between decomposed GRF from both
189 methods and real GRF. They have been normalized to BM.

190

191 **3. Results**

192 In the current study, the absolute error of timing events is 0.003 seconds (SD 0.002).

193 The means (interquartile interval IQ) of the computed Scoeff are presented in Table 1.
194 Their ranges were [0.24;0.72], [-1.03;0.30], [-0.16;0.30], [-0.07;0.31], [-0.05;0.19] and
195 [0.19;1.07] for the anterior force, the lateral force, the vertical force, the frontal moment, the
196 sagittal moment and the transverse moment, respectively.

197 The equations of Scoeff determination from multiple regression are presented in the
198 appendix. Means $RMSE_R$ from both methods are presented in Table 1. Our method allows us
199 to decrease the $RMSE_R$ between 1 and 25% for the GRF and GRM as compared to the Ren's
200 method (Fig. 4).

201

202 PLEASE INSERT TABLE 1

203

204 The mean distances between real CoP and CoP of the both decomposition method in
205 DS were 0.0135 m (IQ 0.007) and 0.0229 m (IQ 0.007) for our method and the Ren's method
206 (Fig. 5), respectively. In double support, the CoP from the Ren's method remained in a
207 constant position. The CoP components was computed from the ratio of GRM and vertical
208 force, their signal shapes being the same from the Ren's method, the CoP stayed in the same
209 position.

210

211 PLEASE INSERT FIGURE 4

212

213 Means of maximum GRF differences normalized to BM are presented in Table 2. Our
214 method compared to the Ren's method decreases the Δ in DS phase by 0.55 N/kg and
215 1.52 N/kg respectively for anterior force and vertical force.

216

217 PLEASE INSERT FIGURE 5

218

219 PLEASE INSERT TABLE 2

220

221 Moreover, the $RMSE_R$'s and the Δ 's IQ of 8 over 9 ground reaction components are

222 higher when computed from the Ren's method than computed using our method (Table 1 and
223 Table 2).

224

225 **4. Discussion**

226 To improve the estimation of ground reaction forces and moments in DS phase, the
227 aim of the study was to enhance the original transition function presented by Ren et al. [8] by
228 including pre-DS ground reaction force characteristics and walking speed, especially as a
229 relationship between ground reaction forces, moments and speed exists [9]. The speed
230 displacement can be a parameter of experimental conditions as can constrained speeds and
231 frequencies. Also, some specific gaits induce lower spontaneous, comfortable and maximal
232 speed, especially in the elderly [14,15], children [16,17] and the obese [18].

233 There are many benefits of using a single force platform. Indeed, it is a simple way to
234 access a lot of information, such as the locomotion phases, the action forces of the whole
235 body and the displacement of the centre of pressure. The method to detect the overground
236 walking DS is inspired from Verkerke et al. [7] and allows us to determine DS events with a
237 3‰ error, according to Roerdink et al. [19]. On the experimental plan, the single force
238 platform configuration avoids us having to worry about the step length of the tested subjects,
239 which is especially useful in i) cases of material constraints, ii) constrained speed and / or
240 step frequency conditions and iii) studying particular gait [14–18].

241 Admitting that the approximation is far from ideal, Ren et al. [8] reported $RMSE_R$ of
242 the walking cycle of 10.9%, 20%, 5.6%, 32.5% 12.2% and 26.2% for the anterior force, the
243 lateral force, the vertical force, the frontal moment, the sagittal moment and the transverse
244 moment, respectively. Our method based on kinetic data of a single force platform enables us
245 to estimate GRF and GRM. Our adaptive transition function induces errors during DS that are
246 lower than the errors during the walking cycle from the original kinematic model [8]. There is

247 a benefit to be gained from being more accurate as to the estimation of the GRF and GRM
248 during the DS phase. First, our method decreases errors to a level lower than intra-individual
249 variability values reported by Winter [20] for anterior and vertical forces (respectively 20%
250 and 7%) whereas the errors from the Ren's method are higher. The errors on GRM and CoP
251 were reduced with our method, hence the errors on lever arm to compute moment using
252 inverse dynamic were reduced. Then, it appears that a best estimation of the CoP, the GRF
253 and the GRM will have a beneficial impact on the computations of net joint torque from the
254 ankle to the hip. Using the both methods to study asymmetries, the maximum GRF
255 differences normalized to BM for anterior and lateral forces in gait cycle are lower than
256 1 N/kg i.e. the minimum difference in GRF parameter values that are biomechanically
257 significant [12]. Our method is the only one that allows us to get maximum vertical GRF
258 difference normalized to BM lower than 1 N/kg (0.73 vs. 2.25). Taking into account the GRF
259 characteristics, our method is adjusted to the step-to-step variability reported by Winter [20].
260 The lower error and variability from our method enable clinicians and researchers to easily
261 highlight statistically significant differences.

262 The difficulties concerning the decomposition methods are to estimate the GRF and
263 GRM in DS phase with the lowest error. A descriptive analysis of errors reveals that mean
264 error and error variability with our method were reduced by more than 50% compared to the
265 Ren's method, except for the lateral force's errors. Our method leads to an error of 3.8% on
266 the vertical force during DS phase. Davis and Cavanagh [2] reported an error on vertical
267 impulse during DS of 1.5% (3.6%, 0.3% and 0.6% for low, medium and high speed,
268 respectively). These errors were computed from one subject who carried out two trials at
269 three different speeds. Robustness and adaptation to the inter-individual variability have not
270 been widely tested. A more recent study [1] reported errors of 3.8% just as our method does.
271 The advantage of our algorithm compared to these of Davis and Cavanagh [2] and Ballaz et

272 al. [1] is that it can be used without accessing the four load cells; also, the decomposition of
273 all GRF and GRM is feasible. Thus a two or three dimensional analysis is possible.

274 From a single force platform, the study of a healthy walking gait along a cycle is
275 feasible by discriminating left and right action force during DS with our method. An accurate
276 estimation of the GRF and GRM during DS associated with a motion analysis system would
277 allow researchers and clinicians to assess all the kinetic parameters during a complete
278 walking cycle. The Scoeff determination equations presented in the Appendix are generics
279 and could be used for all subjects. Further studies are necessary to assess the effects of our
280 method on inverse dynamics calculations and the applicability of our algorithm to
281 pathological gaits.

282

283 **Conflict of interest**

284 None.

285

286 **Acknowledgments**

287 The authors wish to thank David Amarantini and Fabien Dal Maso for their valuable
288 contribution with regard to the expression of the optimization problems.

289

290 **Declarations**

291 **Funding:** This study has been supported by the University of Toulouse 3 that is a public
292 establishment. No private grant has been perceived.

293 **Competing interests:** There is no conflict of interest

294 **Ethical approval:** The subjects have written informed consents approve by the ethic
295 committee of the University of Toulouse 3. This procedure is a simplified one approved when
296 the protocol of the studies are non-invasive

297

298 **References**

- 299 [1] Ballaz L, Raison M, Detrembleur C. Decomposition of the vertical ground reaction
300 forces during gait on a single force plate. *J Musculoskelet Neuronal Interactions* 2013;
301 13: 236-43.
- 302 [2] Davis B, Cavanagh P. Decomposition of Superimposed Ground Reaction Forces into
303 Left and Right Force Profiles. *J Biomech* 1993; 26: 593-7.
- 304 [3] Kram R, Powell A. A Treadmill-Mounted Force Platform. *J Appl Physiol* 1989; 67:
305 1692-8.
- 306 [4] Kram R, Griffin TM, Donelan JM, Chang YH. Force treadmill for measuring vertical
307 and horizontal ground reaction forces. *J Appl Physiol* 1998; 85: 764-9.
- 308 [5] Goldberg SR, Stanhope SJ. Sensitivity of joint moments to changes in walking speed
309 and body-weight-support are interdependent and vary across joints. *J Biomech* 2013;
310 46: 1176-83.
- 311 [6] Potdevin F, Gillet C, Barbier F, Coello Y, Moretto P. Propulsion and Braking in the
312 Study of Asymmetry in Able-Bodied Men's Gaits. *Percept Mot Skills* 2008; 107: 849-
313 61.
- 314 [7] Verkerke GJ, Hof AL, Zijlstra W, Ament W, Rakhorst G. Determining the centre of
315 pressure during walking and running using an instrumented treadmill. *J Biomech*
316 2005; 38: 1881-5.
- 317 [8] Ren L, Jones RK, Howard D. Whole body inverse dynamics over a complete gait
318 cycle based only on measured kinematics. *J Biomech* 2008; 41: 2750-9.
- 319 [9] Nilsson J, Thorstensson A. Ground Reaction Forces at Different Speeds of Human
320 Walking and Running. *Acta Physiol Scand* 1989; 136: 217-27.
- 321 [10] Hamill J, Mcniven S. Reliability of Selected Ground Reaction Force Parameters

- 322 During Walking. *Hum Mov Sci* 1990; 9: 117-31.
- 323 [11] Kristianslund E, Krosshaug T, van den Bogert AJ. Effect of low pass filtering on joint
324 moments from inverse dynamics: Implications for injury prevention. *J Biomech* 2012;
325 45: 666-71.
- 326 [12] Devita P, Bates B. Intraday Reliability of Ground Reaction Force Data. *Hum Mov Sci*
327 1988; 7: 73-85.
- 328 [13] Cahouet V, Martin L, Amarantini D. Static optimal estimation of joint accelerations
329 for inverse dynamics problem solution. *J Biomech* 2002; 35: 1507-13.
- 330 [14] Winter DA, Patla AE, Frank JS, Walt SE. Biomechanical walking pattern changes in
331 the fit and healthy elderly. *Phys Ther* 1990; 70: 340-7.
- 332 [15] Zijlstra A, de Bruin E, Bruins N, Zijlstra W. The step length–frequency relationship in
333 physically active community-dwelling older women - Springer. *Eur J Appl Physiol*
334 2008; 104: 427-34.
- 335 [16] Lythgo N, Wilson C, Galea M. Basic gait and symmetry measures for primary school-
336 aged children and young adults. II: Walking at slow, free and fast speed. *Gait Posture*
337 2011; 33: 29-35.
- 338 [17] Oberg T, Karsznia A, Oberg K. Basic Gait Parameters - Reference Data for Normal
339 Subjects, 10-79 Years. *J Rehabil Res Dev* 1993; 30: 210-23.
- 340 [18] Lai PPK, Leung AKL, Li ANM, Zhang M. Three-dimensional gait analysis of obese
341 adults. *Clin Biomech* 2008;23, Supplement 1:S2-S6.
- 342 [19] Roerdink M, Coolen B, Clairbois BE, Lamoth CJC, Beek PJ. Online gait event
343 detection using a large force platform embedded in a treadmill. *J Biomech* 2008; 41:
344 2628-32.
- 345 [20] Winter D. Kinematic and Kinetic Patterns in Human Gait - Variability and
346 Compensating Effects. *Hum Mov Sci* 1984; 3: 51-76.

APPENDIX

348

349 **Computation of Scoeff for each GRF and GRM and correlation R^2 with the optimized**

350

Scoeff

351 **For antero force F_x ($R^2=0.87$):**

352 $Scoeff = 0.283 - 1.248 \cdot 2T_{ds} - 0.219F_{x_i} - 0.003F_{x_{slope}} + 0.04F_{x_{max}} + 0.03F_{z_i} + 0.002F_{z_{slope}} + 0.034F_{z_{max}}$
 353

354 **For lateral force F_y ($R^2=0.45$):**

355 $Scoeff = 0.691 - 0.312V_F - 2.867 \cdot 2T_{ds} - 0.121F_{x_i} + 0.083F_{x_{max}} + 0.007F_{y_{slope}} + 0.022F_{z_i} - 0.002F_{z_{slope}}$
 356

357 **For vertical force F_z ($R^2=0.8$):**

358 $Scoeff = 0.398 - 0.149V_F - 1.064 \cdot 2T_{ds} - 0.043F_{x_i} + 0.014F_{x_{max}} - 0.036F_{y_{max}} - 0.011F_{z_i} + 0.001F_{z_{slope}}$
 359 $+ 0.026F_{z_{max}}$

360 **For frontal moment M_x ($R^2=0.78$):**

361 $Scoeff = 0.448 - 0.113V_F - 1.08 \cdot 2T_{ds} - 0.05F_{x_i} - 0.001F_{x_{slope}} + 0.018F_{x_{max}} - 0.017F_{z_i} + 0.001F_{z_{slope}}$
 362 $+ 0.029F_{z_{max}}$

363 **For sagittal moment M_y ($R^2=0.74$):**

364 $Scoeff = 0.363 - 0.107V_F - 0.921 \cdot 2T_{ds} - 0.045F_{x_i} - 0.001F_{x_{slope}} + 0.016F_{x_{max}} - 0.017F_{z_i} + 0.001F_{z_{slope}}$
 365 $+ 0.029F_{z_{max}}$

366 **For transverse moment M_z ($R^2=0.64$):**

367 $Scoeff = 0.96 - 2.445 \cdot 2T_{ds} - 0.326F_{x_i} - 0.003F_{x_{slope}} + 0.095F_{x_{max}} + 0.131F_{y_i} + 0.01F_{y_{slope}} + 0.002F_{z_{slope}}$
 368 $+ 0.031F_{z_{max}}$

369 **Transition function (see 2.3)**

370
$$F(t) = F_0 \cdot \left(k_1 \cdot e^{-[(t-t_p)/T_{ds}]^2} - k_2 \cdot \frac{t}{T_{ds}} \right)$$

371 with

372
$$t_p = Scoeff \cdot T_{ds} \quad k_1 = e^{Scoeff^2} \quad k_2 = \frac{1}{2} k_1 e^{-(2 - Scoeff)^2}$$

Table1

RMSE_R assessed on DS (%) and Scoeff values

	Ren's method (IQ)	Our method (IQ)	Scoeff (IQ)
Anterior force	20.62 (13.2)	6.01 (2.8)	0.49 (0.1)
Lateral force	19.05 (17.1)	18.01 (16)	-0.37 (0.3)
Vertical force	11.70 (4)	3.83 (1.5)	0.18 (0.1)
Frontal moment	11.52 (4.1)	4.31 (1.3)	0.18 (0.1)
Sagittal moment	9.17 (3.8)	2.99 (1.5)	0.20 (0.0)
Transverse moment	37.40 (26.4)	12.29 (9.4)	0.54 (0.2)

373

Table 2

Maximum GRF differences normalized to BM (Δ) (N/kg)

	Ren's method (IQ)	Our method (IQ)
Anterior force	0.77 (0.6)	0.22 (0.1)
Lateral force	0.13 (0.1)	0.13 (0.1)
Vertical force	2.28 (0.8)	0.76 (0.3)

374

375 **Figure legends**

376

377 Fig. 1. Example of CoP forward speed minus subject forward speed.

378

379 Fig. 2. The respective contributions of (A) Ren et al. (2008) and (B) the current work brought
380 to the transition functions.

381

382 Fig. 3. Various signal shapes in DS phase with different values of Scoeff. From top to bottom
383 the Scoeff was set at: 1.25, 1, 0.75, 0.5, 0.25, 0, -0.25, -0.5, -0.75, -1 and -1.25.

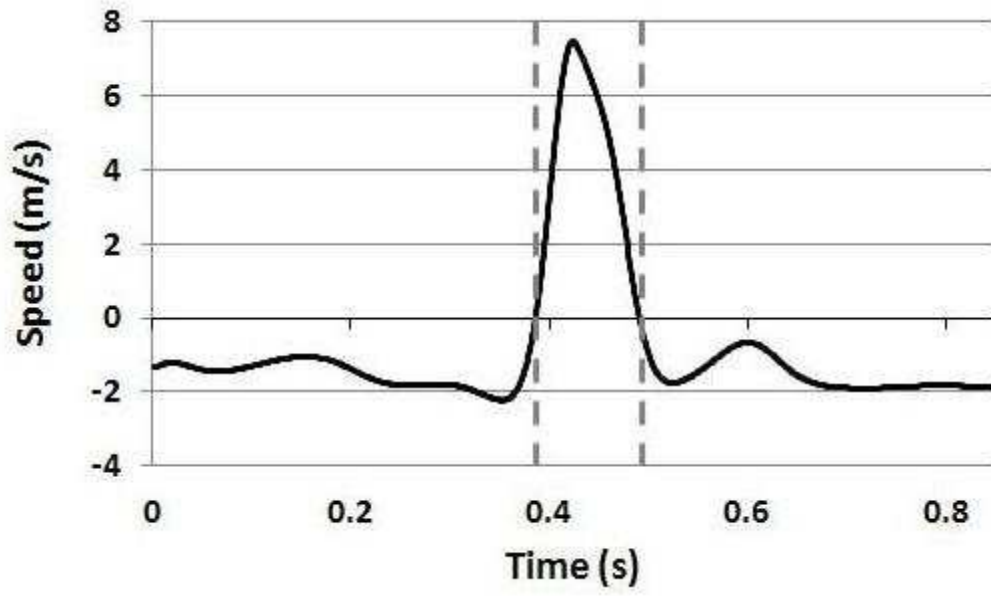
384

385 Fig. 4. Illustration of total GRF and GRM (black line), real GRF and GRM (large gray line),
386 GRF and GRM from our method (black dashed line) and GRF and GRM from Ren's method
387 (black pointed line) for the foot leaving the ground.

388

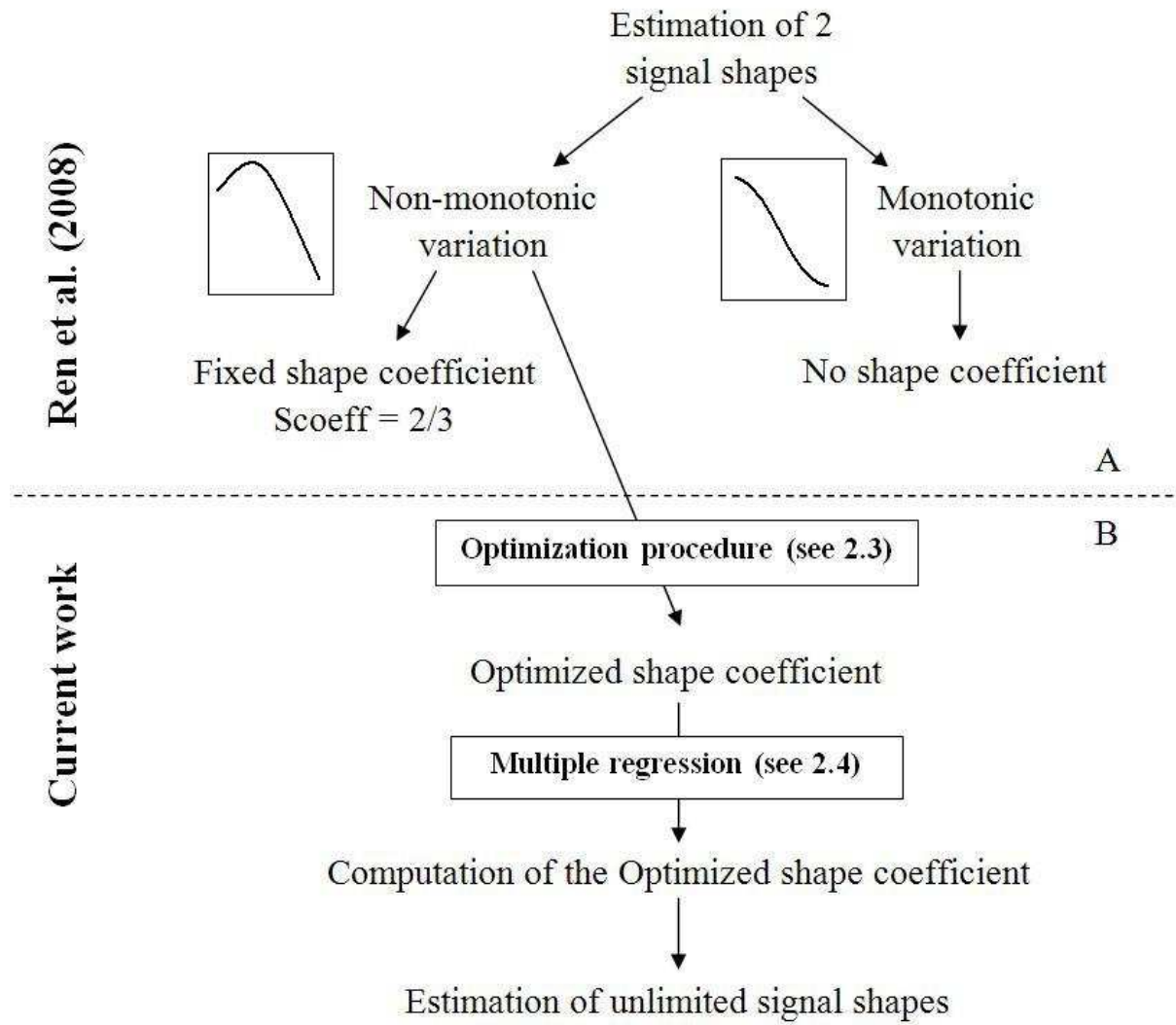
389 Fig. 5. Illustration of the CoP positions on X and Y axis of the experimental coordinate
390 system from real data (large grey line), our method (black dashed line) and Ren's method
391 (black pointed line) under the foot leaving the ground. Vertical lines correspond to the double
392 support beginning.

393

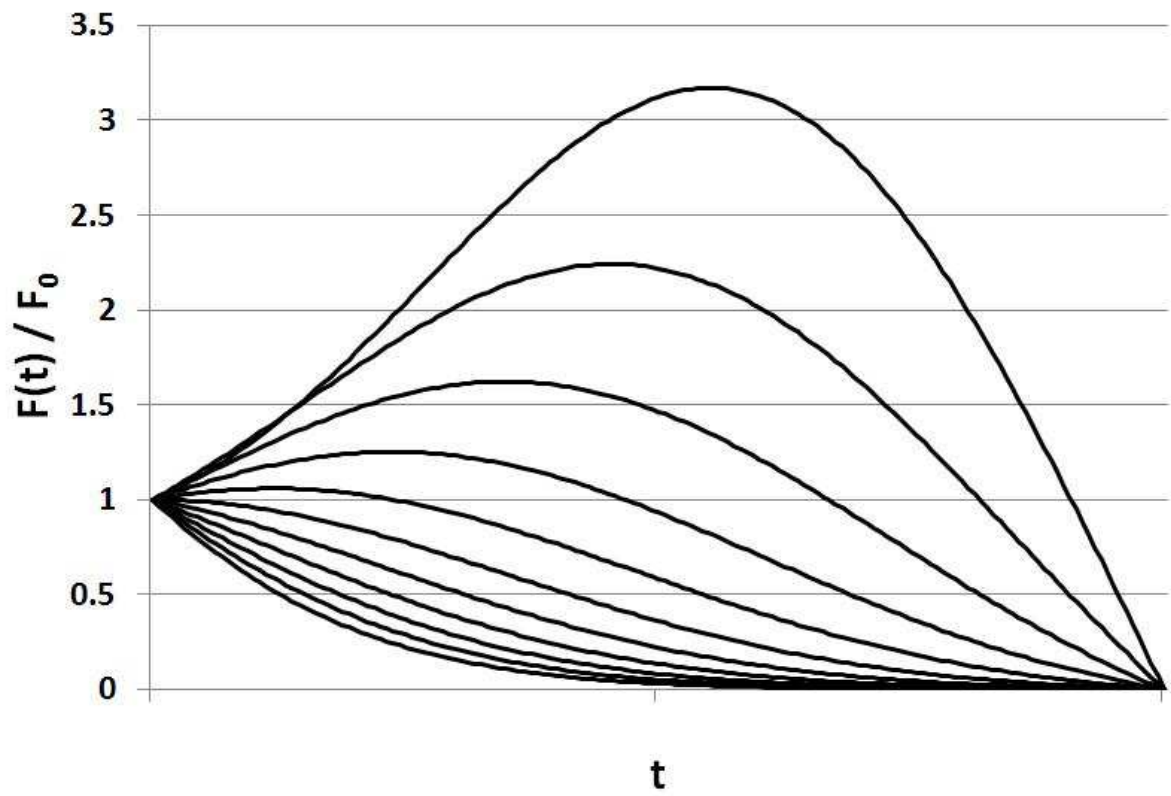


394

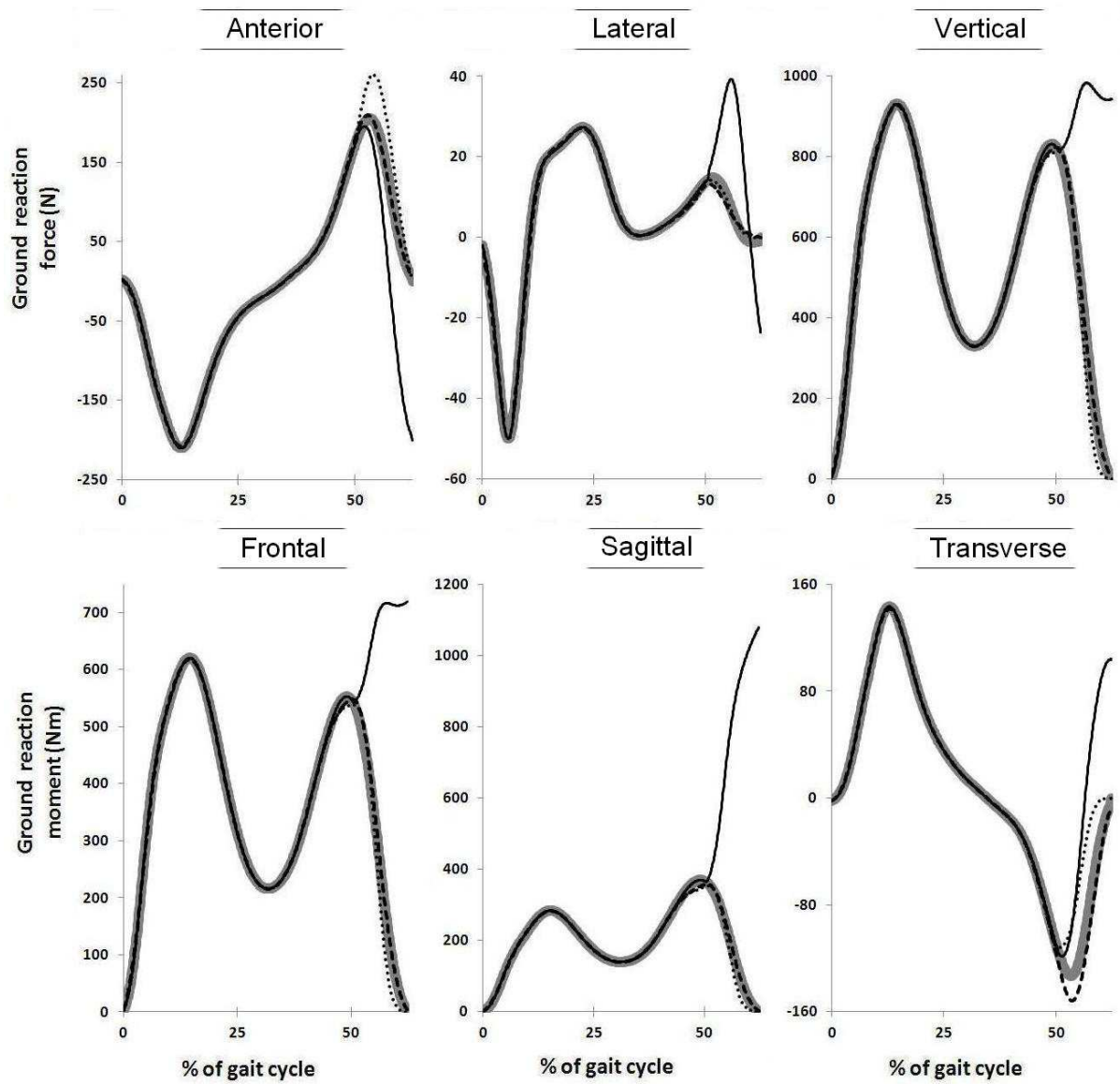
395 Fig. 1



396
397 Fig. 2

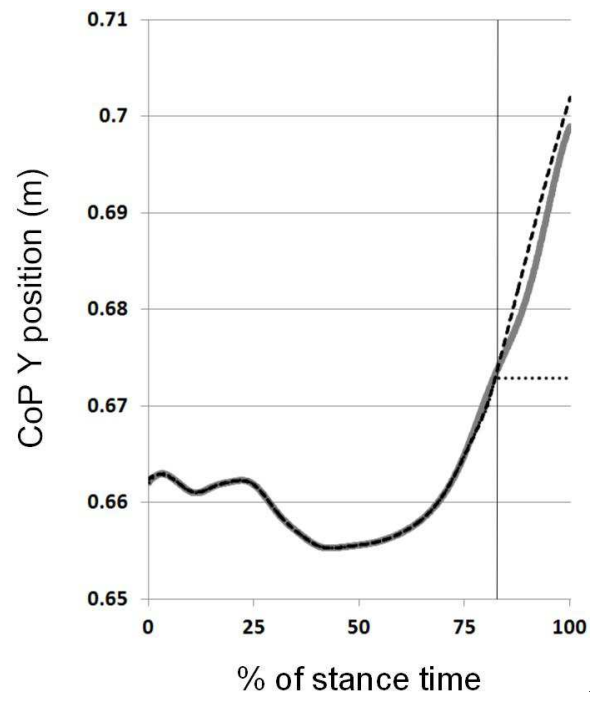
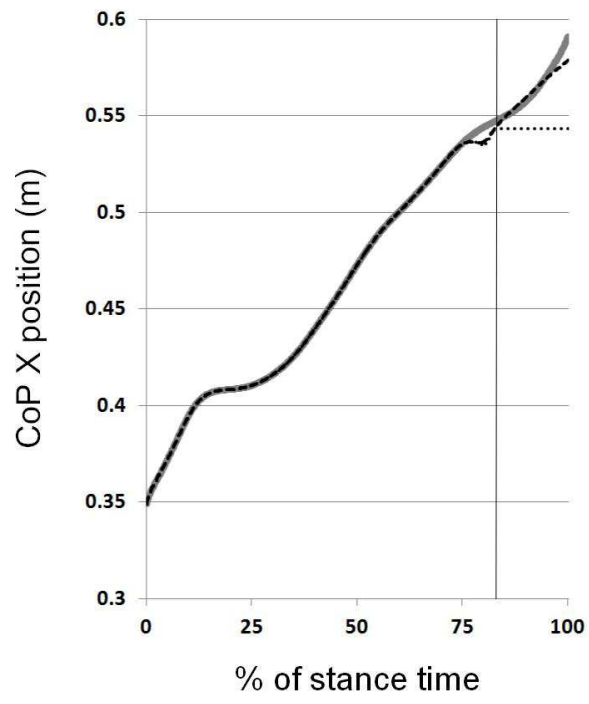


398
399 Fig. 3



400

401 Fig. 4



402

403 Fig. 5